

## Giant Stress Fluctuations at the Jamming Transition

Didier Lootens,<sup>1,2</sup> Henri Van Damme,<sup>1</sup> and Pascal Hébraud<sup>1,\*</sup>

<sup>1</sup>*P.P.M.D., CNRS UMR 7615, ESPCI, 10 rue Vauquelin 75231, Paris Cedex 05, France*

<sup>2</sup>*I.F.P. Division Chimie et Physicochimie Appliquée, 1 avenue de Bois-Préau 92852 Reuil-Malmaison Cedex, France*

(Received 6 December 2002; published 29 April 2003)

We study the stress response to a steady imposed shear rate in a concentrated suspension of colloidal particles. We show that, in a small range of concentrations and shear rates, stress exhibits giant fluctuations. The amplitude of these fluctuations obeys a power-law behavior, up to the apparition of a new branch of flow, leading to an excess of high amplitude fluctuations which exhibit a well-defined periodicity.

DOI: 10.1103/PhysRevLett.90.178301

PACS numbers: 82.70.Dd, 83.60.Rs, 83.80.Hj

When submitted to shear, a concentrated suspension of colloidal particles exhibits a rich variety of behaviors. One of the most striking is of jamming: when sheared above a critical stress, the suspension may stop flowing [1]. This phenomenon is key to many geophysical flows, such as shearing of faults filled with slurries, and is of importance for a number of industrial applications, such as flow of hydrate gas and casting of cement pastes [2]. Numerical simulations [3] and experimental results [4] showed that, at high Péclet numbers, when Brownian forces are negligible compared to shearing forces, the pair distribution function of the particles becomes asymmetric: there is an excess of particle pairs along the compressional axis. Moreover, at high enough volume fractions, many-body interactions play a great role, and the collapse of gaps between particles induces the formation of elongated clusters around the compressional axis of the shear flow [5]. Concentration fluctuations lead to an increase of the viscosity [6] or eventually to the jamming of the suspension [7]. One may thus assume, by similarity with granular materials, that clusters form force chains able to sustain stress along the compressional direction [8]. This implies that, under constant shear rate, strong stress fluctuations associated to building and destruction of these aggregates occur. Such fluctuations have been observed in granular materials [9]. They exhibit long range fluctuations, and the distribution of force fluctuations decreases exponentially with force amplitude [10]. In concentrated suspensions, one may expect a different situation, as, when a shear rate of increasing amplitude is applied, the suspension goes from a low shear rate state, characterized by a low viscosity, to a high shear rate state, highly viscous [11]. In an intermediate shear rate regime, stress fluctuates but is bounded by these two branches of flow.

The aim of this Letter is to describe the statistical properties of stress fluctuations near the jamming transition in a concentrated suspension of monodisperse particles submitted to a constant shear rate.

We used monodisperse silica particles with a diameter ranging from 400 nm to 2.5  $\mu\text{m}$ . They were synthesized

via a Stöber-like synthesis [12]. The size of particles was measured with scanning electronic microscopy. Whatever their size, particle density was 2.1. Stress-imposed measurements were performed with an AR-1000 rheometer. Strain-imposed experiments were done with a Rheometrics RFSII, and we recorded the stress fluctuations. They were performed with a Couette geometry of 17.5 mm outer diameter and 0.25 mm gap. Before each experiment, sample was sheared at 10  $\text{s}^{-1}$  for 1000 s to be placed in a reproducible state. In order to get an accurate enough statistical response in stress time evolution, the stress was measured at a sampling rate of 200 Hz and each experiment lasted for 400 s.

Let us first consider the dynamical phase diagram of a suspension of particles with volume fraction  $\phi$  between 35% and 48% and diameter between 400 nm and 2.5  $\mu\text{m}$  [Fig. 1(a)]. We impose a sinusoidal stress of 1 Hz frequency. At low enough shear stresses, the response is elastic (we will call this phase the “gel phase”). As the stress is increased, the suspension begins to flow (“liquid phase”). We define the transition stress as the value of the stress at which the loss modulus exceeds the elastic modulus. It increases exponentially with volume fraction. When the diameter of the beads is increased, the transition between the gel and the liquid phase occurs at a lower stress. As expected [13], whatever the size of the particles, the transition between the gel and the liquid phases occurs at the same dimensionless stress,  $\sigma a^3/k_B T$ , where  $a$  is the radius of the particles and  $k_B T$  is the thermal energy [Fig. 1(a) inset]. The transition between the gel and liquid phases is thus governed by interparticular forces. In the liquid state, if one does a continuous shear flow experiment, one gets a plastic response; i.e., the stress  $\sigma$  increases as a power law of the shear rate,  $\dot{\gamma}$ :  $\sigma \sim \dot{\gamma}^\alpha$ , where  $0.5 \leq \alpha \leq 1$  increases with the particle size [Fig. 1(b)]. The suspension is thus shear thinning, the smaller the particles, the stronger the shear-thinning behavior. When the amplitude of the stress is further increased, a critical stress appears at which the elasticity sharply increases, and the associated strain becomes extremely noisy. The critical stress at which the moduli

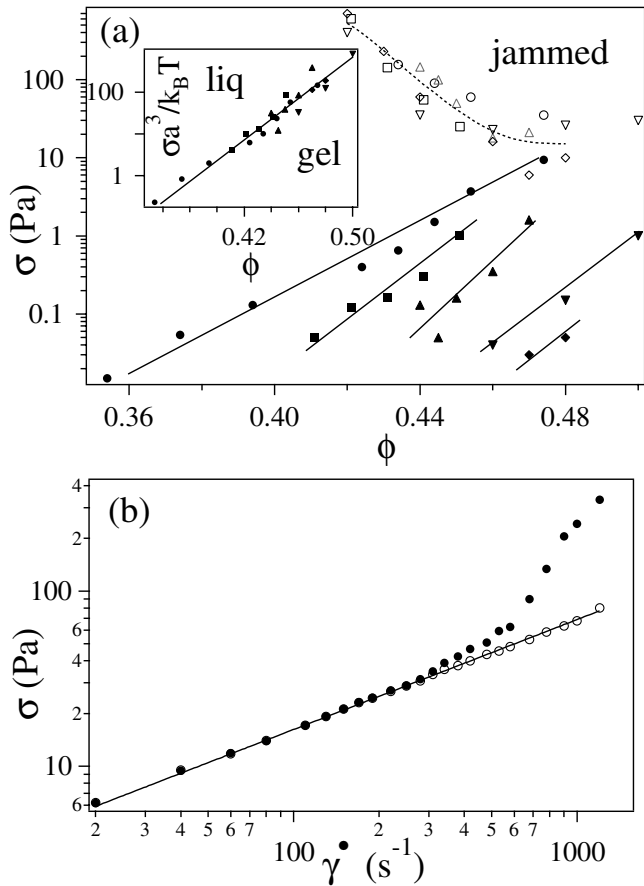


FIG. 1. (a) Dynamic phase diagram for five particle sizes [400 nm (●), 700 nm (■), 1 μm (▲), 1.5 μm (▼), and 2.5 μm (◆)]. Filled symbols delimit the gel from the liquid states, whereas hollow symbols define the liquid from jammed phases boundary. Inset: boundary between the gel and liquid states, in adimensional stress units,  $\sigma a^3/k_B T$ . (b) Stress,  $\sigma$ , vs shear rate,  $\dot{\gamma}$ , for a suspension of 700 nm particles at  $\phi = 43\%$ . Filled symbols are mean stress values, and hollow symbols are stress most probable values (they cannot be distinguished from each other for  $\dot{\gamma} \leq 300 \text{ s}^{-1}$ ). The line is a power-law fit of the average stress in the liquid regime, leading to  $\sigma \propto \dot{\gamma}^{0.63}$ .

increase defines a new transition, from the shear-thinning liquid regime to a jammed state. Jamming appears at lower stress (or strain) when the volume fraction increases. At high concentration of particles, the liquid domain disappears, and it becomes impossible to distinguish between the gel and the jammed phase. Within experimental uncertainties, the boundary between liquid and jammed states does not change when the size of the particle varies [Fig. 1(a)] and cannot be rescaled the same way as the stress at the gel/liquid boundary was. This implies that the stress at which jamming transition occurs does not rely upon thermal fluctuations on the length scale of the particles, but that jamming is essentially a geometrical transition, governed by the free volume of the suspension.

Let us now apply a constant shear rate. In the “liquid” phase, the stress is well defined and fluctuates around a mean value, with Gaussian noise of small amplitude [Fig. 2(a)]. Then, when one reaches the transition shear rate between the liquid and the jammed states, the stress distribution is no longer Gaussian but assumes an extreme-value distribution statistics. Nevertheless, the probability distribution function of the stress exhibits a well-defined maximum. The most probable stress value continuously increases as  $\dot{\gamma}$  is increased while the amplitude of the fluctuations increases [Fig. 1(b)]. It thus exists a well-defined low-viscosity branch of flow from which fluctuations develop. The amplitude of the largest fluctuations may be 10 times higher than the most probable stress value. The stress distribution function exhibits a very long power-law tail [Fig. 2(b), from  $\dot{\gamma} = 190$  to  $780 \text{ s}^{-1}$ ]. At higher strain rates, the fluctuations are cut

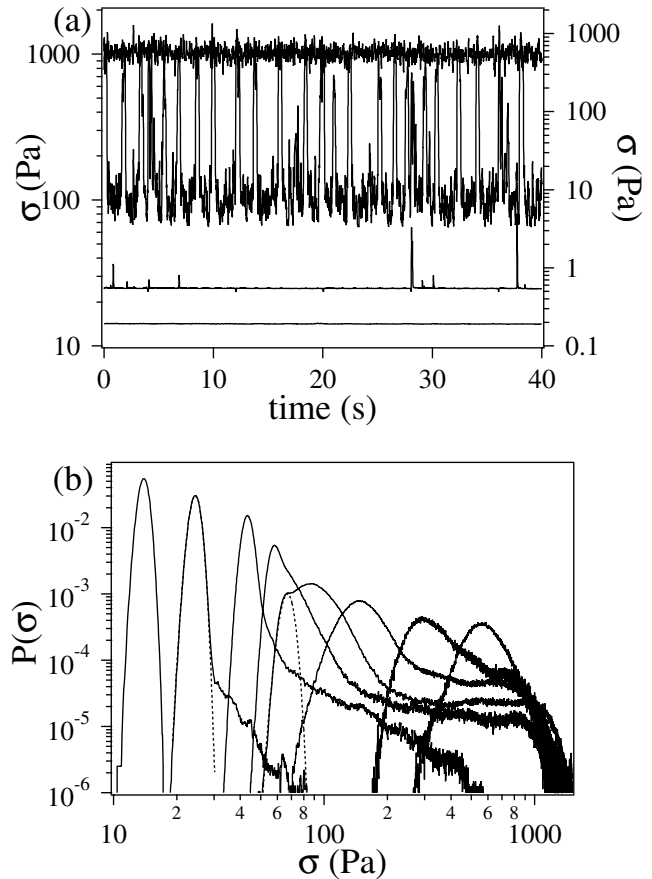


FIG. 2. (a) Time evolution of stress for four different imposed shear rates (from bottom to top: 80, 190, 1000, and 2200  $\text{s}^{-1}$  (right axis)) of 700 nm particles at a volume fraction of 43%. For  $\dot{\gamma} = 1000 \text{ s}^{-1}$ , we indicate the mean stress value and the width of the Gaussian noise. (b) Probability distribution functions of stress for different shear rates (left to right: 80, 190, 480, 780, 1000, 1200, 1400, 2200  $\text{s}^{-1}$ ). The fit of the Gaussian fluctuations is indicated on the 190 and 1000  $\text{s}^{-1}$  curves (dashed line).

off by a high viscosity branch of flow. This flow regime is characterized by large stress fluctuations symmetric around a mean value. Huge fluctuations of well-defined amplitude develop between the two flow regimes ( $\dot{\gamma} \geq 1000 \text{ s}^{-1}$ ). One may thus consider two different classes of fluctuations: critical fluctuations of widespread amplitude, leading to a long tail of the stress distribution function, on one hand, and fluctuations of well-defined amplitude between the two branches of flow on the other hand. As we have observed that the most probable stress state continuously evolves at the jamming transition [Fig. 1(b)], these high fluctuations may be unambiguously separated from Gaussian noise. Let us thus define a peak as a stress fluctuation whose amplitude is larger than the most probable stress value increased by twice the width of the Gaussian fluctuations. Each of these peaks defines an event during which a given amount of energy is dissipated. The density of energy released per unit volume during one peak is given by

$$E = \int_{\text{peak}} [\sigma(t') - \sigma_{\text{max}}] \dot{\gamma} dt', \quad (1)$$

where  $\sigma_{\text{max}}$  is the most probable stress. Whereas the average energy released by critical fluctuations,  $E_0$ , increases when the shear rate amplitude increases (Fig. 3 inset), the probability distribution of released energies exhibits (Fig. 3) a power-law behavior,  $P(E) \propto E^{-2}$ , over a wide range of strain rates,  $680 \text{ s}^{-1} \leq \dot{\gamma} \leq 1400 \text{ s}^{-1}$ . The system thus behaves as a critical system, where energy fluctuations occur on every scale. Nevertheless,

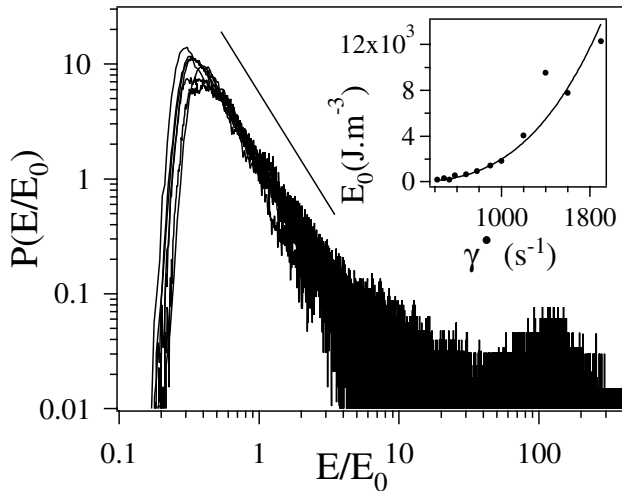


FIG. 3. Probability distribution functions of the energy released by stress fluctuations for several shear rates (380, 480, 580, 680, 780, 900, and  $1000 \text{ s}^{-1}$ ) of 700 nm particles at a volume fraction of 43%. Energy is rescaled by the mean released energy,  $E_0$ . The straight line is a power law of slope  $-2$ . Inset: mean released energy,  $E_0$ , as a function of shear rate,  $\dot{\gamma}$ . The line is a guide to the eye.

the tuning of the control parameter,  $\dot{\gamma}$ , does not have to be accurate, and we observe this power-law distribution of energies over a wide range of values of  $\dot{\gamma}$ . In that sense, the situation is very similar to what is observed in self-organized critical systems. The flow regime exhibits here strong analogies with the flow of granular materials, where energy is released during avalanches of widespread amplitudes, and whose size probability distribution function obeys a power law. But a second branch of flow, corresponding to a “grinding flow,” develops. This leads to a dynamical instability and gives birth to giant fluctuations, leading to an excess of high energy peaks (Fig. 3) whose temporal properties are of interest.

Let us consider now the temporal properties of the stress fluctuations and the distribution of peaks lifetimes. This distribution exhibits two distinctive features [Fig. 4(a)]: a decaying behavior at short times, and a long time peak, corresponding to the lifetime of the fluctuations between the two branches of flow.

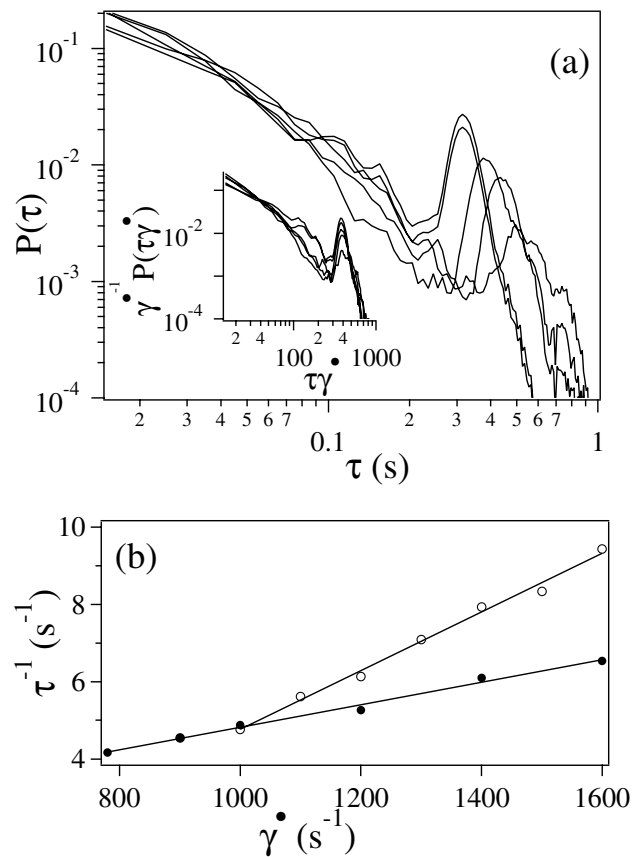


FIG. 4. Lifetime distributions of fluctuations (700 nm particles at a volume fraction of 43%) for five different shear rates,  $\dot{\gamma} = 780, 900, 1000, 1200, 1400 \text{ s}^{-1}$ . Inset: probability distribution functions of lifetimes rescaled by the shear rates,  $\dot{\gamma}$ . (b) Inverse of the lifetime fluctuations vs shear rate, for 700 nm (respectively,  $2.5 \mu\text{m}$ ) particles at  $\phi = 43\%$  ( $\bullet$ ) (respectively,  $\circ$ ). The straight line is a linear fit leading to  $\gamma_c = 2.85 \times 10^4\%$  (respectively,  $\gamma_c = 1.32 \times 10^4\%$ ).

We are not able to define a characteristic law for the short time fluctuations, but the long characteristic lifetimes  $\tau$  of the fluctuations are very well defined and decrease when  $\dot{\gamma}$  is increased. They obey  $\tau = \gamma_c / \dot{\gamma}$  [Fig. 4(b)], and one may thus define a characteristic shear amplitude,  $\gamma_c$ , that does not depend on the shear rate. In other words, whatever the shear rate, a transition between the two branches of flow occurs when the system has been sheared by  $\gamma_c$ .

The characteristic deformation defined by one period of the fluctuation is  $\gamma_c = 2.85 \times 10^4\%$  for 700 nm particles and  $\gamma_c = 1.32 \times 10^4\%$  for 2.5  $\mu\text{m}$  particles. These fluctuations thus define a very long length scale, of the order of a fraction of the deformation corresponding to an entire rotation of the cylinder (which corresponds to  $\gamma = 4.33 \times 10^4\%$ ). Similar fluctuations have been observed in shear-thickening surfactant solutions [14] and onion-phase surfactants [15]. They were in both cases associated to a phase transition under flow. A model of “rheochaos” has been recently proposed, which accounts for strain fluctuations under a controlled stress [16]. Assuming the existence of strain inhomogeneities inside the material, and under the hypothesis that high-strained regions possessed a higher modulus than low-strained regions, the authors showed that a positive feedback coupling between the dynamics of low-strained regions and high-strained regions occurred, leading to an instability characterized by well-defined oscillations. The high values of  $\gamma_c$  observed here are at odds with the results of this model, which predicts that the characteristic deformation of the fluctuations should be of the order of unity. This implies that there must exist, in our case, a macroscopic length scale much higher than the diameter of the particle, and of the order of the largest size of our system. We have checked that this behavior was not a property of the Couette geometry but remained in plate/plate geometries of various gaps. The origin of this length scale was not elucidated. One may assume it is linked to the travel of an aggregate along the circumference. We have also observed that the normal stress induced close to the jamming transition fluctuates in phase with the tangential stress. Solid friction thus plays a dominant role in the dynamics of the system. The main feature of the observed dynamics—the existence of two well-defined classes of fluctuations—may thus be due to the role played by solid friction between particles. Indeed, the Burrige-Knopoff model of sliding blocks exhibits very similar properties. In this model, a chain of blocks attached to each other by a spring and to a fixed surface by leaf springs is put in

contact with a rough surface moving at a constant speed [17]. Localized motions of the blocks whose statistics obeys a power-law distribution occur. These small movements smooth the heterogeneities of relative positions of neighboring blocks, which are put on the verge of slipping by the moving rough surface, thus leading to an excess of large delocalized motions involving the whole system [18]. This behavior is very similar to the distribution of energy relaxation events we observed. Thus, a concentrated suspension of colloidal particles under flow appears to be a very simple model system that exhibits some essential features of self-organization, which are key to understanding the complex flow of many concentrated dispersions.

We thank É. Lécolier for many fruitful discussions.

---

\*Electronic address: pascal.hebraud@espci.fr

- [1] R. S. Fall, J. R. Melrose, and R. C. Ball, *Phys. Rev. E* **55**, 7203 (1997).
- [2] J. Mewis, *J. Non-Newtonian Fluid Mech.* **6**, 1–20 (1979).
- [3] J. F. Brady and J. F. Morris, *J. Fluid Mech.* **348**, 103–139 (1997).
- [4] F. Parsi and F. Gadala-Maria, *J. Rheol.* **31**, 725 (1987).
- [5] J. F. Brady and G. Bossis, *J. Fluid Mech.* **155**, 105 (1985).
- [6] R. L. Hoffman, *Trans. Soc. Rheol.* **16**, 155–173 (1972).
- [7] E. Bertrand, J. Bibette, and V. Schmitt, *Phys. Rev. E* (to be published).
- [8] M. E. Cates, J. P. Wittmer, J.-Ph. Bouchaud, and P. Claudin, *Phys. Rev. Lett.* **81**, 1841 (1998).
- [9] B. Miller, C. O’Hern, and R. P. Behringer, *Phys. Rev. Lett.* **77**, 3110 (1996).
- [10] S. N. Coppersmith, C.-H. Liu, S. Majumdar, O. Narayan, and T. A. Witten, *Phys. Rev. E* **53**, 4673 (1996).
- [11] W. J. Frith, P. d’Haene, R. Buscall, and J. Mewis, *J. Rheol.* **40**, 531–548 (1996).
- [12] W. Stöber and A. Fink, *J. Colloid Interface Sci.* **26**, 62–69 (1968).
- [13] W. B. Russel, D. A. Saville, and W. R. Schowalter, *Colloidal Dispersions* (Cambridge University Press, Cambridge, 1989).
- [14] R. Bandyopadhyay and A. K. Sood, *Europhys. Lett.* **56**, 447–453 (2001).
- [15] A. S. Wunenberger, A. Colin, J. Leng, A. Arnéodo, and D. Roux, *Phys. Rev. Lett.* **86**, 1374 (2001).
- [16] D. A. Head, A. Ajdari, and M. E. Cates, *Europhys. Lett.* **57**, 120 (2002).
- [17] R. Burrige and L. Knopoff, *Bull. Seismol. Soc. Am.* **57**, 341 (1967).
- [18] J. M. Carlson, J. S. Langer, B. E. Shaw, and C. Tang, *Phys. Rev. A* **44**, 884 (1991).